



β -Cyclodextrin-epichlorohydrin polymer/graphene oxide nanocomposite: preparation and characterization

Abolfazl Heydari^{1,2} · Hassan Sheibani² · Viktor Hronský³ · Ivica Janigová¹ · Miroslav Šlouf⁴ · Peter Šiffalovič⁵ · Ivan Chodák¹

Received: 17 August 2017 / Accepted: 20 December 2017 / Published online: 13 January 2018
© Institute of Chemistry, Slovak Academy of Sciences 2018

Abstract

In this study, we report a novel and simple technique to synthesize water-insoluble nanocomposite macromolecule composed of graphene oxide (GO) nanosheets and β -cyclodextrin (β -CD) polymer. These nanocomposites were synthesized by the one-pot precipitation polymerization process via polycondensation of β -CD with epichlorohydrin (ECH) in an aqueous suspension of GO under alkaline condition. The obtained β -CD polymer/GO (CDP-ECH/GO) were characterized by thermal gravimetry, differential scanning calorimetry, infrared and Raman spectroscopies, high-resolution solid state ¹³C NMR, X-ray diffraction, electron microscopy (both SEM and TEM), and energy dispersive spectroscopy. Furthermore, the mechanism of CDP-ECH/GO nanocomposites formation is also discussed depending on the type of mixing device that has been used during polymerization. The swelling ratio of the nanocomposites as well as their absorption properties toward methylene blue (MB), phenol (PN), 1-naphtol (1-NPH) and 2-naphtol (2-NPH) have been determined. Increasing the GO content in the nanocomposites results in an increase of the adsorption capacity of the materials.

Keywords β -Cyclodextrin · Graphene oxide · Hydrogels · Nanocomposites · Adsorption

Introduction

Carbohydrate macromolecules (polysaccharides) attract the interest of researchers especially as they represent an important group of biopolymers. Since monosaccharides have multiple functional groups, polysaccharides can form linear polymers (e.g., cellulose) or complex branched structures (e.g. glycogen) (Namazi et al. 2012). Polysaccharides

perform numerous roles in living organisms, acting as energy stores such as starch and as structural components such as chitin in arthropods.

Among carbohydrate macromolecules, β -CD (a derivative of starch) have appealed significant interest in a broad range of applications, because of their good biocompatibility, high biodegradability, the presence of various functional groups and notable capacity to form inclusion complexes with other materials through host–guest interactions (Fenyvesi et al. 2005; Heydari et al. 2015, 2016, 2017a; Namazi and Heydari 2014; Namazi et al. 2014). Nowadays, several methods have been developed to produce carbohydrate macromolecules by polymerization of β -CD. The β -CD polymers have been successfully employed in both industrial applications and background research such as water treatment, separation processes, food additives, packaging materials, environmental science, textile industry, cosmetics, tissue engineering and drug delivery (Heydari et al. 2017b, c; Liu et al. 2014, 2016; Mocanu et al. 2001; Namazi and Heydari 2014; Namazi et al. 2014; Singh et al. 2002). At present, considerable attention is paid to investigation of the removal of pollutants from wastewater using β -CD polymers (Heydari et al. 2017b; Liu et al. 2014; Morin-Crini and Crini 2013).

✉ Abolfazl Heydari
heydaria86@gmail.com

✉ Hassan Sheibani
hsheibani@uk.ac.ir

¹ Polymer Institute of the Slovak Academy of Sciences, 845 41 Bratislava, Slovakia

² Department of Chemistry, Shahid Bahonar University of Kerman, Kerman 76169, Iran

³ Department of Physics, Technical University of Košice, Park Komenského 2, 042 00 Košice, Slovakia

⁴ Institute of Macromolecular Chemistry, Academy of Sciences of the Czech Republic, 162 06 Prague, Czech Republic

⁵ Institute of Physics of the Slovak Academy of Sciences, 845 11 Bratislava, Slovakia

For direct separation and purification purposes, it is, therefore, required to produce water-insoluble β -CD polymers by polymerization reactions or by immobilizing the β -CD molecules on a solid support using grafting (Alsaiee et al. 2016; Heydari and Sheibani 2015; Namazi et al. 2014). For this aim, the main type of water-insoluble β -CD polymer was synthesized using epichlorohydrin (ECH) as a crosslinker. ECH is the most frequently investigated crosslinking agent for β -CD, and the reaction between these two species is the most straightforward method for environmental applications (Morin-Crini and Crini 2013). Nowadays, properties of the β -CD polymer can be modified, including stability to heat, shear forces, and ability to capture of guests. Two effective ways are described in the literature, namely either chemical modification or integration of β -CD polymer with other materials to form polymer composites (Heydari et al. 2016, 2017c; Heydari and Sheibani 2015, 2016; Namazi and Heydari 2014; Namazi et al. 2014).

The discovery of polymer nanocomposites has opened a novel dimension in the field of material science. So far, numerous nanofillers have been used in the preparation of polymer nanocomposites. Among them, graphene oxide (GO) is known as a basis for the new type of carbon nanomaterials, which has attracted scientific interests due to its excellent thermal, mechanical and electrical properties (Allen et al. 2010; Eom et al. 2009; Lee et al. 2008; Yan et al. 2017). The GO has a large number of oxygen groups, such as hydroxyl, epoxide and carboxyl groups (He et al. 1998; Lorf et al. 1998). Therefore, this compound behaves like an amphiphilic macromolecule with hydrophilic edges and a hydrophobic basal plane. Unlike oxidation processes of other carbonaceous materials, GO preparation is considerably cost-effective (Chen et al. 2012a; Hummers and Offeman 1958) and offers the potential for large-scale production. Moreover, in comparison to other carbon-based nanomaterials, GO seems to be an environmentally friendly material including biocompatibility (Chen et al. 2012b). This compound has attracted vast potential application not only in mechanics (Lee et al. 2008) and electronics (Eom et al. 2009) but also in wastewater treatment (Guo et al. 2015a; Zhao et al. 2011b). It has been used for the adsorption of fluoride ions (Li et al. 2011), heavy metals (Deng et al. 2010; Mishra and Ramaprabhu 2011; Yang et al. 2010a), dyes (Gaffar et al. 2004; Prabaharan and Mano 2006; Ramesha et al. 2011) and expresses a good adsorption property.

In the last decade, the research on graphene nanosheets/ β -CD hybrid increased significantly in many fields such as electrocatalysis and electrochemical sensors (Guo et al. 2010, 2011a, b; Liu et al. 2011, 2012; Tan et al. 2010; Xu et al. 2011). The β -CD-functionalized graphene nanosheets are frequently used for molecule detection, e.g., dopamine, doxorubicin, methotrexate and phenolic organic pollutants. Lately, we reported on a water-insoluble β -CD polymer/GO

and β -CD polymer/reduced graphene oxide nanocomposites. These nanocomposites were synthesized in the presence of citric acid as a crosslinker through in situ melt polymerization. These compounds reveal higher electrochemical response toward uric acid, dopamine and tyrosine (biomolecules) in comparison with unmodified β -CD polymer (Heydari and Sheibani 2016).

Following our previous works in preparation of β -CD polymers and their nanocomposites (Heydari et al. 2016, 2017b, c; Heydari and Sheibani 2015, 2016; Namazi and Heydari 2014; Namazi et al. 2014), the current study focuses on the preparation of CDP-ECH/GO nanocomposites using a one-pot precipitation polymerization process with ECH as crosslinker. The CDP-ECH/GO nanocomposites are synthesized by nucleophilic addition reaction between hydroxyl groups of β -CD and GO with ECH under alkaline condition. Also, in particular the influence of reaction conditions and GO content on the interaction between GO, β -CD and ECH has been investigated in the prepared nanocomposites structure. Then, the structure and swelling behavior of resulting nanocomposites were investigated by general methods. In this study, we have also investigated the influence of the GO content on the absorption of four model molecules such as methylene blue (MB), phenol (PN), 1-naphthol (1-NPH) and 2-naphthol (2-NPH).

Experimental

Chemicals

Natural graphite powder (Fluka), β -CD (SDFCL, Mumbai), potassium permanganate (KMnO_4 , Merck), sodium nitrate (NaNO_3 , Merck), epichlorohydrin (ECH, Sigma-Aldrich), sulfuric acid (H_2SO_4 , Merck), hydrochloric acid (HCl, Merck), ethanol (Merck), methylene blue (MB, Merck), phenol (PN, Merck), 1-naphthol (1-NPH, Merck), 2-naphthol (2-NPH, Merck), hydrogen peroxide (H_2O_2 , Mojallali, Iran) and sodium hydroxide (NaOH, Mojallali, Iran) were all purchased and used as received. Deionized water was used throughout all experiments.

Synthesis of graphene oxide

Graphite oxide was prepared by oxidizing pristine graphite according to the modified Hummer's method (Heydari and Sheibani 2016; Hong et al. 2012; Hummers and Offeman 1958). The achieved graphite oxide was suspended in water (1 mg per 1 mL of water) and exfoliated to GO nanosheets by using a titanium-alloy solid probe ultrasonicator (20 kHz, 400 W, Topsonic, Iran) set at 40% intensity with 10 s/10 s ON/OFF pulses and a total of 2 h ON time. The achieved GO dispersion was then subjected

to centrifugation to remove any unexfoliated GO which is usually present in a rather small amount. Finally, the suspension was lyophilized with a Zirbus Freeze Drying System to avoid collapse of the structure.

Synthesis of CDP-ECH/GO

Water-insoluble CDP-ECH/GO nanocomposites were synthesized applying two procedures as described below. The GO content was chosen as 0.3, 0.6, 1.2 and 2.4 (wt%).

Path-1

In a thermostated reactor vessel, 3 g of β -CD was mixed with 3 mL of GO solution. The ECH (2.1 mL) was added at 50 °C with stirring during 4 min. The mixing was performed under either sonication and magnetic stirring (Path 1–1) or only magnetic stirring (Path 1–2) to achieve a homogeneous suspension. Then, 2.3 mL of aqueous NaOH (40% w/w) was added dropwise under constant stirring at 50 °C during 45 min. It was observed that the viscosity of the solution started to increase and a solid gel was formed (Fig. 1a). The obtained solid gel was broken into particles, soaked in 50 mL of water and stirring continued for 1 h while cooling the product down to ambient temperature. The alkaline medium was neutralized with HCl aqueous solution and the product was washed numerous times with ethanol and water. At last, soaked nanocomposites in water were lyophilized with a Zirbus Freeze Drying System. The final pure CDP-ECH/GOs were obtained as dark solids (Fig. 1b).

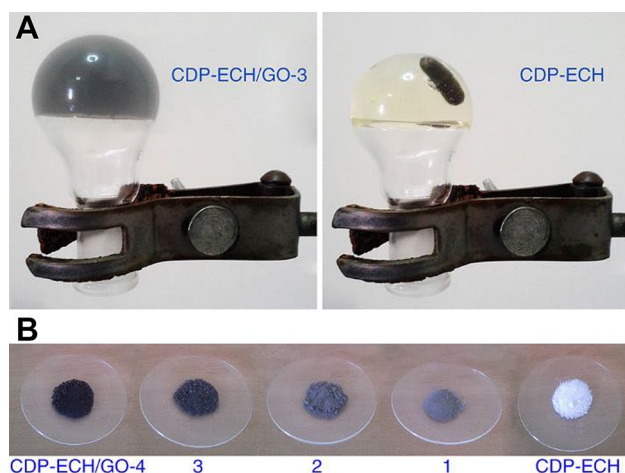


Fig. 1 **a** Photographs of CDP-ECH and CDP-ECH/GO-3 gels formed during reaction. **b** Photographs of CDP-ECH, CDP-ECH/GO-1, 2, 3 and 4 nanocomposite powders

Path-2

3 g of β -CD and 3 mL of GO solution were mixed. ECH (2.1 mL) was gradually added at 50 °C during stirring for 4 min. The mixture was mixed under magnetic stirring to achieve a homogeneous GO suspension. 0.6 mL of aqueous NaOH solution (40% w/w) was added dropwise under constant stirring at 50 °C during 15 min. The solution was carried out under sonication for 30 min. Then, 1.7 mL of the aqueous NaOH solution was added dropwise during 30 min. It was observed that the viscosity of the solution gradually increased until a solid gel was formed. Then, the solid gel was purified using the procedure described for Path 1. The final pure CDP-ECH/GO was obtained as a dark solid.

Synthesis of CDP-ECH

For comparison, β -CDP-ECH (β -CD polymer without GO) was also prepared as previously described (Garcia-Zubiri et al. 2006) with some modifications. 6 g of β -CD and 6 mL of water was mixed. 4.2 mL of ECH was added into the solution and the obtained mixture was stirred. 4.2 mL of aqueous NaOH was added dropwise under permanent stirring at 50 °C during 45 min. The obtained solid gel (Fig. 1a) was purified using the procedure described for Path 1. The final pure CDP-ECH was obtained as a white solid (Fig. 1b).

Characterization of materials

Thermal analysis

Thermogravimetric measurements (TGA), differential thermogravimetric analysis (DTG), differential scanning calorimetry (DSC) and differential of differential scanning calorimetry (DDSC) were performed on a 409 PG Netzsch (Germany) instrument. Approximately 15 mg of the materials were heated from 50 to 800 °C at a heating rate of 15 °C/min under nitrogen atmosphere (flow rate of 50 mL/min). Deconvolution of the DTG analysis curves was performed by Origin Lab 2017 software and Gaussian bases.

ATR-FTIR analysis

The Fourier transform Infrared (FT-IR) (Brucker Tensor 27) spectra of the prepared materials were measured at ambient temperature by attenuated total reflection (ATR) mode.

High resolution solid state ^{13}C NMR

The ^1H - ^{13}C CP MAS NMR measurements were performed on a Varian 400 MHz NMR spectrometer (Palo Alto, CA, USA). The high-resolution ^{13}C NMR spectra were recorded at a resonance frequency of approximately 100 MHz with

the use of 4 mm ZrO₂ rotors and MAS frequency of 10 kHz at ambient temperature. The spectra were recorded under CP condition with ¹H 90° pulse of 2,8 μs, contact time of 2 ms, acquisition time of 20 ms, SPINAL pulse high power proton decoupling of 90 kHz, recycle delay of 8 s, and averaging over 9000 scans. Chemical shifts were referenced to tetramethyl silane using adamantane as an external standard. The spectra were processed using MestReNova software.

Raman spectroscopy

The Raman measurements were performed on confocal Raman microscope (alpha300 R+, Witec, Germany) using 50 × objective (NA = 0.8), laser excitation line 532 nm and effective confocal pinhole size of 100 μm. The mean Raman spectrum was calculated by averaging of 2.500 spectra collected from an area of 10 × 10 μm². The CCD integration time for single spectrum was set to 200 ms.

XRD patterns

X-ray diffraction (XRD) patterns were achieved on a Phillips X'Pert PRO equipped with CuKα radiation (λ = 1.54178 Å) under a voltage of 40 kV.

FE-SEM and EDS analyses

The surface morphology of lyophilized materials was obtained by field emission-scanning electron microscopy (FE-SEM, Sigma, Zeiss). The pictures were taken at an excitation voltage of 15 kV. The local elemental composition of the nanocomposites was determined by energy dispersive spectroscopy (EDS) analysis with an EDAX Oxford instruments attached to the SEM column.

TEM analysis

Transmission electron microscopy (TEM) analysis was performed at a Zeiss EM10C (Germany) instrument using an acceleration voltage of 100 kV, to observe the dispersion of GO sheets within the polymer matrix. The nanocomposites were firstly dispersed in water and the samples were prepared by dropping diluted nanocomposites on the Lacey support grid and dried in a vacuum oven at ambient temperature.

Swelling properties

The classical gravimetric method was used to determine swelling behavior of the materials. The dried materials (ca. 0.15 g) were immersed in water at 25 °C for selected time intervals. The swelled materials were removed from the water and then were weighed after the water on the surface

was carefully and quickly wiped. The swelling ratio (g/g) of the materials was calculated as follows:

$$W = \frac{(W_d - W_s)}{W_s} \times 100$$

where W is the swelling ratio of materials, W_s and W_d are the weight of the materials before and after swelling, respectively.

Adsorption test

The adsorption studies were conducted by batch equilibrium method. The CDP-ECH or CDP-ECH/GOs (0.1 g) were mixed with 50 mL of MB, PN, 1-NPH and 2-NPH solutions in glass flasks and the suspensions were stirred for 1, 1.5, 2.5 and 2.5 h, respectively, at 25 °C. After achieving the adsorption equilibrium, the adsorbents were separated from the solution by centrifugation. The concentrations of MB, PN, 1-NPH and 2-NPH remnants in the solution were recorded by a UV–Visible spectrophotometer (Cary50; Varian, Australia) at 664 nm, 270 nm, 322 nm and 328 nm, respectively. The removal percentage was calculated using the following equation:

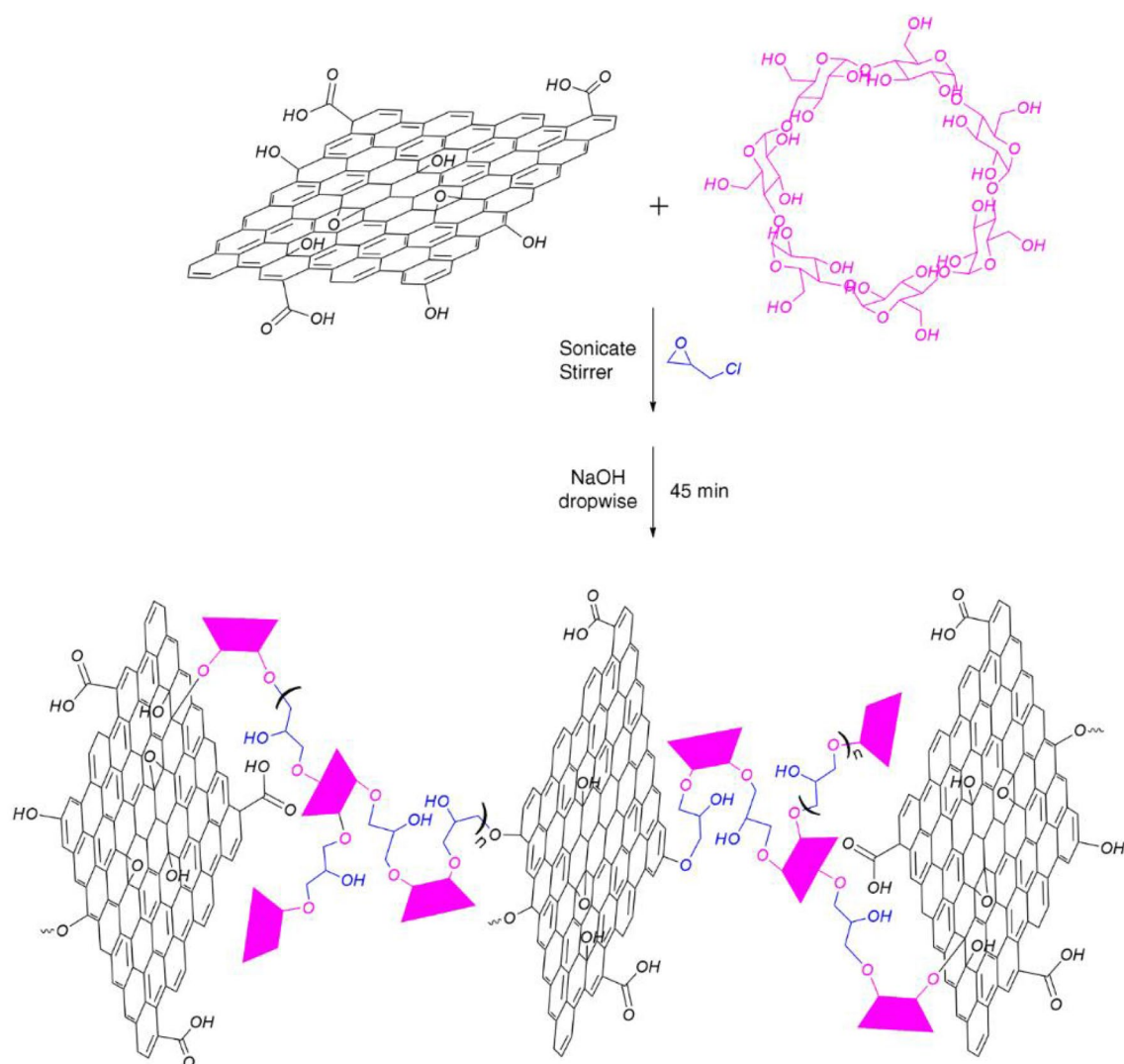
$$\text{Removal (\%)} = \left(\frac{C_0 - C_e}{C_0} \right) \times 100$$

where C_0 is initial concentration of sorbates (mg/L); and C_e is equilibrium concentration of sorbates, which was calculated according to calibration curves.

Results and discussion

Synthesis conditions

The synthesis process of CDP-ECH/GO is shown in Scheme 1. The CDP-ECH/GO nanocomposite networks were prepared using pristine β-CD as building block, GO nanosheets as nanofiller and ECH as crosslinker. The β-CD contains various number of hydroxyl groups with different reactivity in two faces. The primary hydroxyl groups of the β-CD cavity (OH-6) is often more nucleophilic than the two secondary hydroxyl functions (OH-2 and OH-3), which represent the main drawback when polymerization is concerned. The order is OH-6 > OH-2 > OH-3 (Loftson and Brewster 1996). The OH-6 (pK_a being 15–16) is more basic than the OH-2 and OH-3 (pK_a ~ 12), so the weak and strong alkaline conditions can be a reason for different reactivity of those. It is well known that under high alkalinity (high NaOH concentration) most of the substitution reactions occur on one side of this cavity (primary face), while under low alkaline pH (NaOH < 5 wt%), only



Scheme 1 Schematic illustration of the one-pot preparation of CDP-ECH/GO nanocomposites

the most acidic hydroxyl groups (OH-2 and OH-3) turn to anions; so the substitution reactions occur on the two sides (Pitha et al. 1990; Renard et al. 1997). On the other hand, on the surface of GO many functional groups exist such as hydroxyls (pK_a 9.8) and carboxyls (pK_a 4.3 and 6.6) (Chen et al. 2013), which provide the anionic charge necessary for the nucleophilic reactions, and also epoxy groups (C–O–C) which are known as the appropriate sites for the electrophilic reactions. Many studies have shown that ECH reacts with hydroxyl groups of GO under alkaline conditions which not only increases the chemical activity of GO surface but also provides suitable binding arms (Chen et al. 2016; Guo et al. 2015b; Liu et al. 2013; Qi et al. 2017; Wang et al. 2016).

In this research, to deprotonate all of the hydroxyl groups in the β -CD and GO, we gradually increased the concentration of NaOH to allow the hydroxyl groups of GO (Chen et al. 2016; Guo et al. 2015b; Liu et al. 2013;

Qi et al. 2017; Wang et al. 2016) and β -CD with lower nucleophilicity to react with ECH. Therefore, during the synthesis procedure, ECH interacted with hydroxyl functional groups on the GO surface to yield nanocomposite with the covalent linkage between GO and CDP-ECH. Another important factor for this reaction is accessibility of hydroxyl groups beside the ECH in starting reaction when concentration of NaOH is low. In this case, the hydroxyl groups with lower reactivity on β -CD and GO can also react with ECH. Therefore, we can conclude that the final structure depends on the conditions of mixing of starting materials in this reaction. For this purpose, three conditions were chosen to perform these reactions; details are shown in Table 1. The products including a mixture of crosslinked β -CD and GO joined by repeating glyceryl units of polymerized ECH have been prepared (Scheme 1).

Table 1 Different reaction conditions were used for the preparation of nanocomposites

	Sample code	GO content (wt%)	Reaction conditions	Yield (%)
Path 1–1	CDP-ECH/GO-1	0.3	A mixture of β -CD, GO and ECH carried out under sonication and magnetic stirring, then NaOH was added	85
	CDP-ECH/GO-2	0.6		86
	CDP-ECH/GO-3	1.2		84
	CDP-ECH/GO-4	2.4		74
Path 1–2	CDP-ECH/GO-P1–2	1.2	A mixture of β -CD, GO and ECH carried out under magnetic stirring, then NaOH was added	72
Path 2	CDP-ECH/GO-P2	1.2	One portion of NaOH was added to the mixture of β -CD, GO and ECH then sonicated and finally additional NaOH amount was added	74

TGA and DTG analyses

Evidence for the effect of GO content and reaction condition on the structure of nanocomposites have been verified by the DTG analysis. For this purpose, DTG curves and deconvolution computation of these curves from Origin software into its two constituent peaks of CDP-ECH, CDP-ECH/GO-1, 2, 3 and 4, and also CDP-ECH/GO-3 CDP-ECH/GO-P1–2 and CDP-ECH/GO-P2 (Fig. 2) have been compared. Figure 2 shows DTG and deconvoluted DTG curves of pure CDP-ECH and its nanocomposites obtained by Path 1–1 with different amount of GO. Deconvoluted DTG curves show that there are two decomposition temperatures in the CDP-ECH. One mass loss due to decomposition of ECH polymer units is around 320 °C, and the other is at approximately 374 °C, which is related to the β -CD decomposition (Pratt et al. 2010). As depicted in Fig. 2, the height of peak appearing at 320 °C decreases along with the increase of the GO content in the nanocomposites. The reason for this effect should be due to the preparation of β -CD polymer nanocomposites with GO as a nanofiller, and in the case of CDP-ECH/GO-3, a highly homogeneous composite was obtained if compared to other nanocomposites. Based on these results, the other reaction conditions for testifying the mixing effect were chosen for nanocomposites obtained by Path 1–1, Path 1–2 and Path 2 and loaded 1.2% GO. For this aim, the DTG curves of CDP-ECH/GO-3, CDP-ECH/GO-P1–2 and CDP-ECH/GO-P2 have been compared (Fig. 2). From a comparison of curves, it is concluded that the achieved CDP-ECH/GO-3 by Path 1–1 which in initial the β -CD, GO and ECH mixture are well homogenized by sonicating and stirring exhibit better results compared to the two other methods.

Owing to the satisfactory results achieved for composite obtained by Path 1–1, further investigations were performed with product prepared by this method. TGA analysis of CDP-ECH, CDP-ECH/GO-1, 2, 3 and 4 have been performed and results are presented in Fig. 3. Pure CDP-ECH and its nanocomposites exhibit two main steps of weight loss in TGA curve. The first step ranging from

50 to 190 °C is due to a dehydration process of the water in these rather hydrophilic polymers. The second weight loss ranging from ~ 190 to 400 °C is assigned to the decomposition of β -CD polymer. No noticeable changes occurred in TGA curves of nanocomposites due to existence of the groups with similar decomposition behavior, but there are only shifts in second weight loss along with increase of GO content, which are consistent with the results obtained from DTG analysis.

DSC and DDSC analyses

Figure 4a, b illustrate DSC and DDSC curves of CDP-ECH, CDP-ECH/GO-1, 2, 3 and 4. It is well known that the DSC curve of a crystalline β -CD reveals two endothermic peaks which have appeared at its decomposition around 320 °C (Namazi and Heydari 2014). In the DSC curve of CDP-ECH, an endothermic peak appeared at about 296 °C that confirmed the formation of CDP-ECH from β -CD. As shown in Fig. 4a, DSC records of the CDP-ECH/GO-1 and 2 contain an exothermic peak of the polymer decomposition without noticeable changes compared to CDP-ECH, which indicate preparation of composite with prevailing phase of CDP-ECH units. Based on the DSC curves of CDP-ECH/GO-3 and CDP-ECH/GO-4, the temperature peaks related to decomposition of polymer unit were shifted to higher temperature after mixing with GO. This phenomenon should be due to the preparation of the nanocomposites in which the interactions between the β -CD polymer and GO exist with improved stability that corresponds to the results of DTG and TGA. The DDSC curves of nanocomposites that are shown in Fig. 4b are consistent with the results, which were obtained from DSC.

ATR-FTIR analysis

Fourier-transform infrared spectroscopy was used to obtain the information about the interactions between CDP-ECH and GO nanosheets. Figure 5 represent the ATR-FTIR

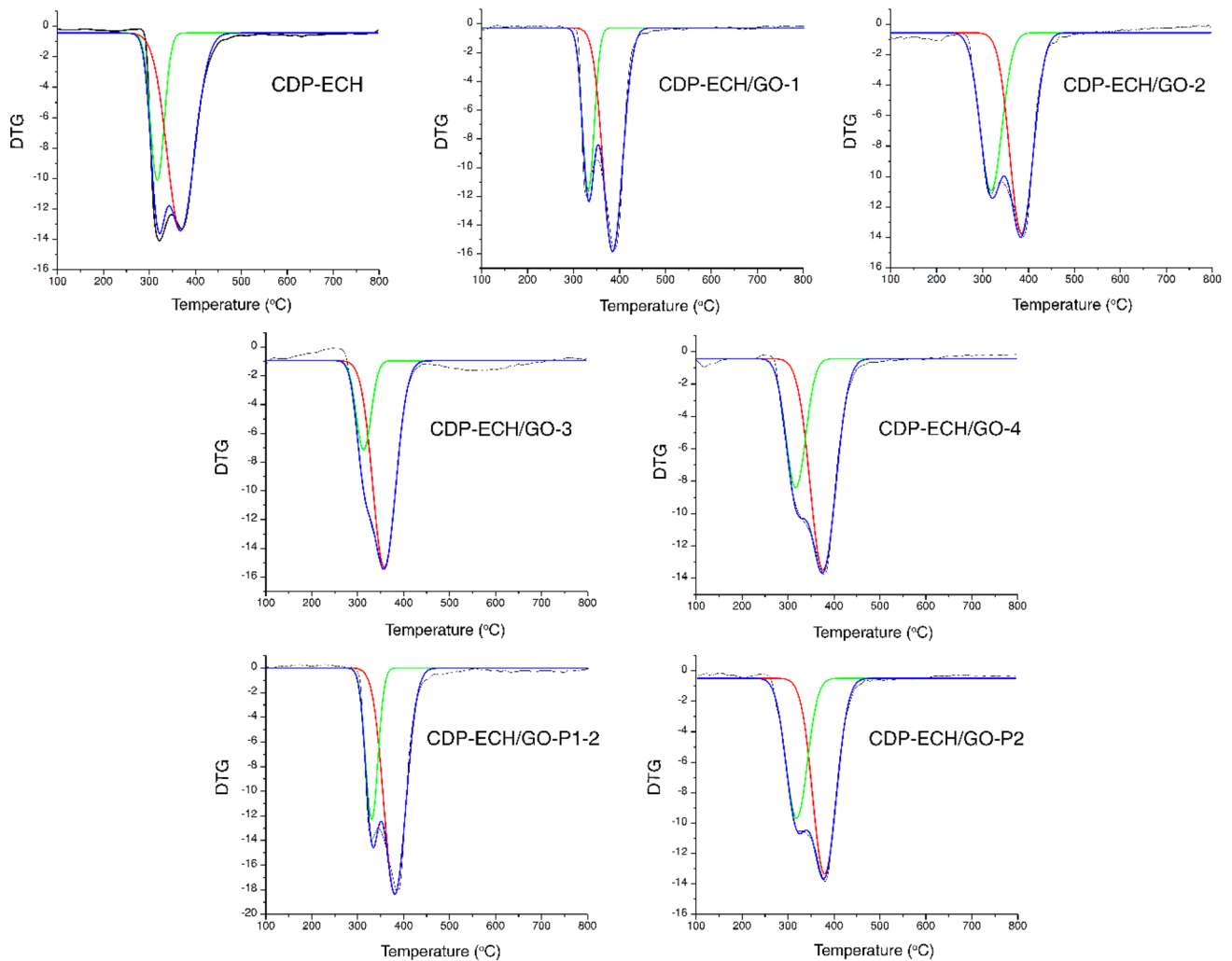


Fig. 2 DTG curves of CDP-ECH, CDP-ECH/GO-1, 2, 3 and 4, CDP-ECH/GO-P1-2 and CDP-ECH/GO-P2 along with deconvolution computation of these curves using Origin software into two constitu-

ent peaks. Black: experimental DTG; Blue: simulated DTG curve (almost the same as the black curves); Green and Red: calculated peaks from the deconvolution computation with Origin software

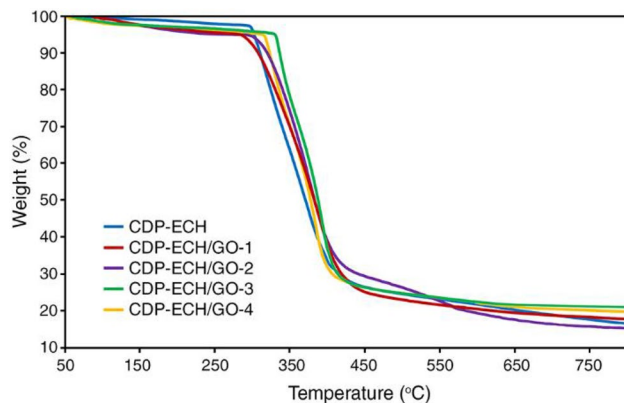


Fig. 3 TGA curves of CDP-ECH, CDP-ECH/GO-1, 2, 3 and 4

spectra of GO, CDP-ECH, CDP-ECH/GO-1 and CDP-ECH/GO-3. The IR spectra of these compounds revealed a strong absorption at 3400 cm^{-1} attributed to the OH groups and the stretching and bending vibrations of C–H bands at $2925\text{--}2880$ and $1480\text{--}1280\text{ cm}^{-1}$, respectively. In addition, the stretching vibrations of C–O bands at $1030\text{--}1139\text{ cm}^{-1}$ and other adsorption peaks in the spectrum of CDP-ECH appeared nearly at the same wavenumbers in the spectra of CDP-ECH/GO-1 and 3. The similar peak-shaped vibration of CDP-ECH and CDP-ECH/GOs implies that the nanocomposites keep the original characteristic structure of CDP-ECH. However, the typical adsorption peaks of GO at 3407 , 1734 and 1225 cm^{-1} indicate the presence of hydroxyl, carboxylic and epoxy groups, respectively. These peaks were absent in the spectra of CDP-ECH/GOs, due to be possibly overlapped by other peaks, except the peak at 1734 cm^{-1} which appears in nanocomposites as a shoulder and confirms

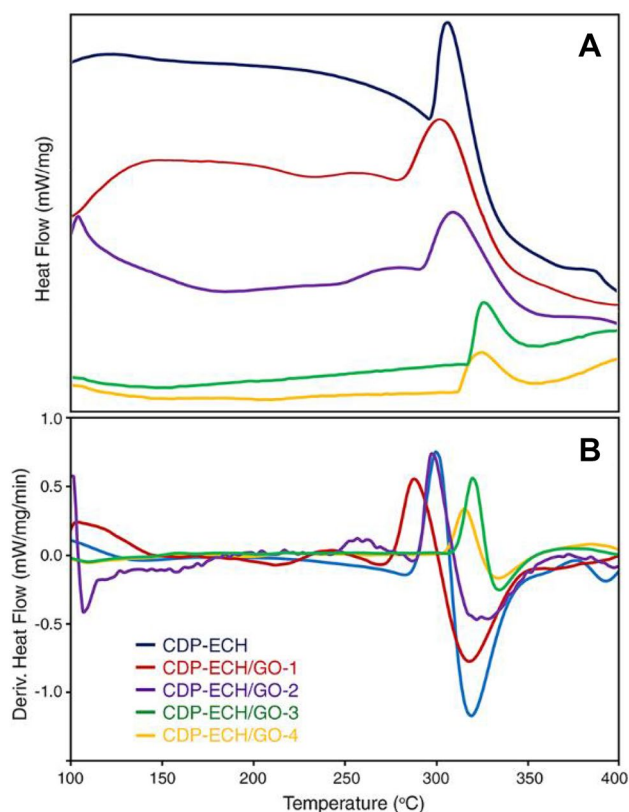


Fig. 4 a DSC and b DDSC curves of CDP-ECH, CDP-ECH/GO-1, 2, 3 and 4

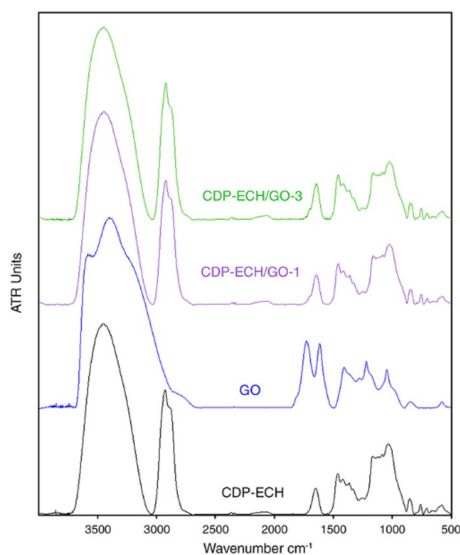


Fig. 5 ATR-FTIR spectra of CDP-ECH, GO, CDP-ECH/GO-1 and 3

the presence of the C=O stretching vibration of GO. These results provide more evidence for the successful chemical functionalization. According to the previous report, O–H stretching vibration in nanocomposites could be shifted to

a lower wavenumber through formation of hydrogen bond between polymer and GO (Yang et al. 2010b), whereas, here shifts to the CDP-ECH/GO structure are not seen. It may indicate the presence of the covalent bonds between β -CD, GO nanosheets and ECH.

Solid-state ^{13}C NMR analysis

NMR analysis was carried out by solid-state CP MAS ^{13}C NMR technique and the spectra measured for the CDP-ECH, CDP-ECH/GO-3 and 4 are depicted in Fig. 6. In the spectrum of CDP-ECH, the resonances at range 50–110 ppm are assigned to the C1–C6 carbons of the β -CD moiety (C1—104.4 ppm, C4—81 ppm (as a shoulder), C2, 3, 5—around 72 ppm, C6—62.2 ppm) and of the glyceryl bridge carbons connecting β -CD cavities (Crini et al. 1998; Heydari et al. 2016). A small sharp peak at 63.9 ppm is attributed to the CH_2OH carbons of the epichlorohydrin. In the single pulse MAS ^{13}C NMR spectrum of GO, three carbon resonances at 130, 68 and 57 ppm assigned to non-oxygenated (sp^2), C–OH and C–O–C carbons, respectively, were reported (Stankovich et al. 2007). Generally, all peaks mainly appear as broad single peaks. No chemical shift changes were observed in the spectra for CDP-ECH and its nanocomposites after reaction of CDP-ECH with GO, which is probably due to the overlapping of the new carbon peaks obtained from the linkage between the polymer and GO with the carbon peaks of CDP-ECH. But not even carbon resonances of GO were observed in the CP MAS ^{13}C NMR spectra measured for CDP-ECH/GO nanocomposites. The absence of carbon resonance of GO could be due to the fully covered GO sheets by networks of β -CD polymer which indicates that the nanocomposites have been formed. However, it is also possible that this absence is on account of too small amounts of GO in nanocomposites and of very weak ^{13}C NMR signal of

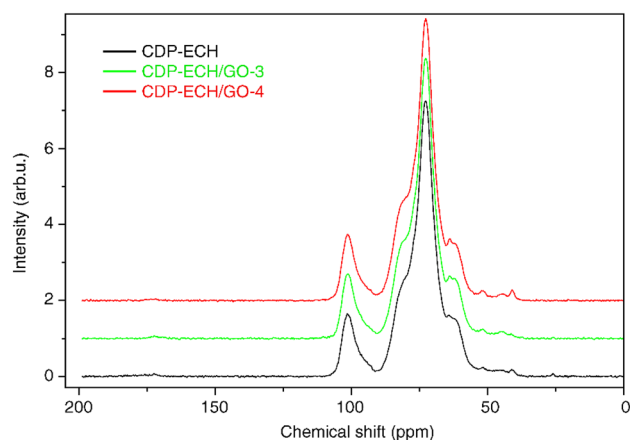


Fig. 6 CP MAS ^{13}C NMR spectra of CDP-ECH, CDP-ECH/GO-3 and 4

GO (Stankovich et al. 2007). In spite of no new peaks were observed in the NMR spectra measured for nanocomposite samples, as compared with that of CDP-ECH, there is a notable change of the shape of the spectra for nanocomposite samples (Fig. 6). A better resolution of the C4 signal at 81 ppm as well as enhancement of carbon signals from the region of 40–60 ppm is observed which according to (SDBS Spectral Database for Organic Compounds <http://sdb.sriod.b.aist.go.jp>) corresponds to epichlorohydrin. Changes mentioned above indicate the formation of the CDP-ECH/GO nanocomposites.

Raman spectroscopy

The Raman spectra of β -CD polymer and GO-nanocomposites are shown in Fig. 7. All samples conjugated with GO display D and G Raman bands located at 1355 and 1590 cm^{-1} , respectively. A broad 2D band of GO near 2700 cm^{-1} is visible as well. The structural defects, edges and functional groups of GO flakes activate the energy dispersive D band. The most prominent Raman band of pure β -CD polymer belongs to symmetric and asymmetric CH stretches and is located at 2800–3000 cm^{-1} . This particular Raman band is visible in all measured samples and confirms a presence of both β -CD polymer and GO in the nanocomposites. The other visible Raman bands include CH deformation (1430–1480 cm^{-1}), C–C and C–O single bonds (near 1100 cm^{-1}), vibration band of glucose ring at 938 cm^{-1} and broad OH band between 3100 and 3600 cm^{-1} .

XRD patterns

Figure 8 shows the XRD patterns of the CDP-ECH/GO-1, CDP-ECH/GO-3, CDP-ECH and GO. The graphite revealed

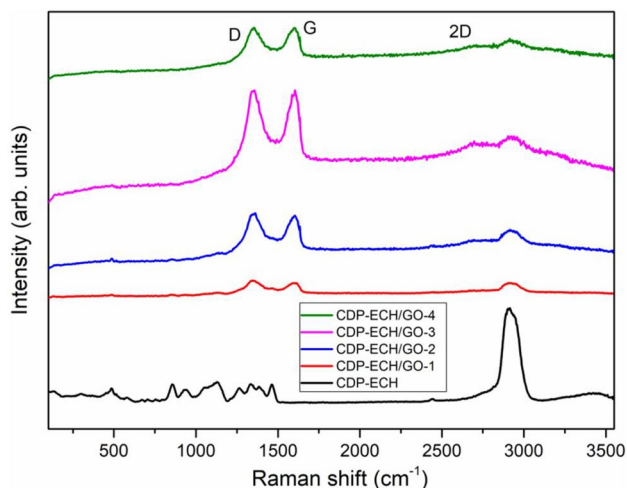


Fig. 7 Raman spectra of CDP-ECH, CDP-ECH/GO-1, 2, 3 and 4

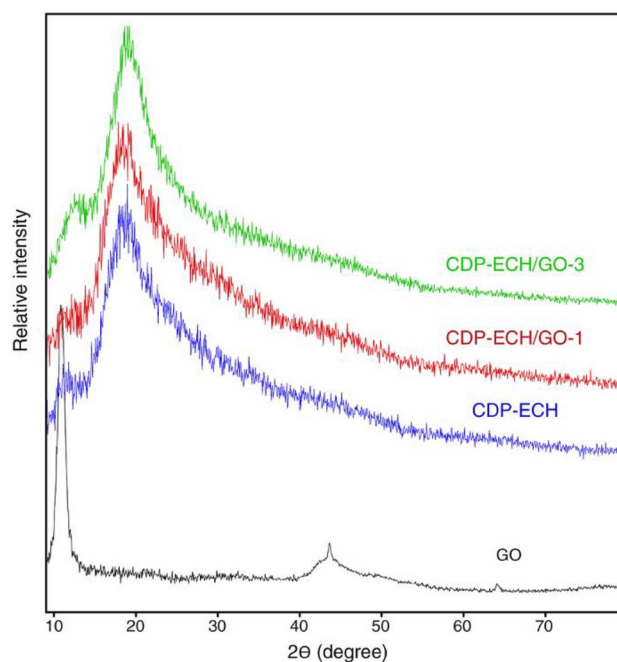


Fig. 8 XRD patterns of GO, CDP-ECH, CDP-ECH/GO-1 and 3

a peak at 26.33° (a d -spacing of 0.33 nm) (Zhao et al. 2010), while after oxidation and sonication, this peak disappears completely and another peak appears at 10.78° (a d -spacing of 0.85 nm) which confirms the successful preparation of GO nanosheet in agreement with the references (Yang et al. 2011). For the pure CDP-ECH, a broad peak is seen at around 19.5°, which corresponds to the amorphous pattern of the β -CD polymer. The amorphous pattern appears due to high crosslinking degree between β -CD and ECH. The XRD patterns of the polymer nanocomposites prepared using linking of GO with CDP-ECH (Fig. 8) show only the diffraction peak of CDP-ECH while the peak related to GO disappeared. Finally, these results exhibit that GO particles were fully exfoliated into single sheets in the achieved polymer nanocomposites.

FE-SEM and EDS analyses

The GO, CDP-ECH, CDP-ECH/GO-1 and CDP-ECH/GO-3 were characterized using FE-SEM (Fig. 9a) to determine the resulting polymer surface and dispersion of GO in the β -CD polymer. The CDP-ECH including numerous β -CD units in its structure appears as porous with different pore size, regular-shaped and extremely smooth, which might be intimately related to presence of crosslinked polymer networks. While β -CD consists of irregular three-dimensional particles with a parallelogram shape (Lee et al. 2006) this result reveals that the CDP-ECH was successfully synthesized. As seen in Fig. 9a, CDP-ECH/

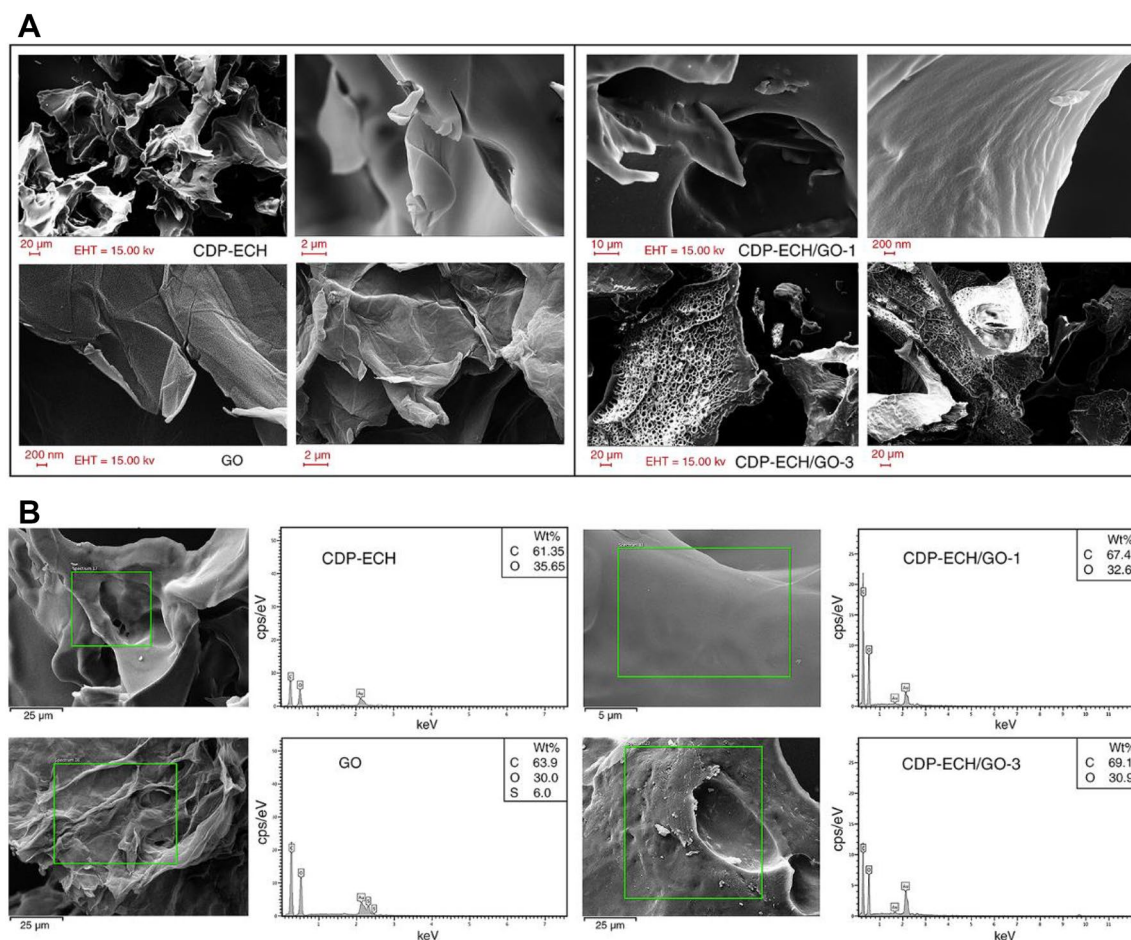


Fig. 9 a FE-SEM images and b EDS data of the CDP-ECH, GO, CDP-ECH/GO-1 and 3

GO-1 and 3 retained their original shape and structure of CDP-ECH, containing well distributed and homogenized nanolayers of GO in the composite.

The local chemical composition of GO, CDP-ECH, CDP-ECH/GO-1 and CDP-ECH/GO-3 has been estimated from EDS measurements. As seen in Fig. 9b, only the elements C (62.85%) and O (37.15%) are present in pure CDP-ECH. The performed EDS on GO indicates the presence of C (63.9%), O (30.1%) and S (6.0%). The EDS of CDP-ECH/GO-1 and CDP-ECH/GO-3 also show only the presence of C (67.4 and 69.1%), and O (32.6 and 30.9%), respectively, and hence confirm the high purity of prepared polymer nanocomposites. Compared with the EDS spectrum of CDP-ECH, the increase in the content of C and decrease in the amount of O confirms the existence of GO nanofiller in the CDP-ECH/GOs. Moreover, EDS spectrum of CDP-ECH/GO-3 shows an increase in the content of C and the decrease of O elements in comparison with CDP-ECH/GO-1, confirming an increase of GO amount in CDP-ECH/GO structure along with the increase of primary GO (if considering all chemical composition similar to local chemical composition).

TEM analysis

Transmission electron microscopy imaging was used to supplementary investigation of the graphene oxide morphology inside the β -CD polymer. It has to be stated that the observation was rather difficult especially due to powdery nature of the materials which required the observation in dispersion in a solvent which was consequently fixed to a carbon fibre network. Therefore, higher magnification was impossible to perform because of extensive heating of the sample leading to evaporation and hindrances regarding focusing. The TEM images which we were able to collect of CDP-ECH and its nanocomposites with different loadings amount of GO are shown in Fig. 10. The TEM images illustrate the flake-like shapes of CDP-ECH and its nanocomposites, which corrugated and scrolled like crumpled silk veils. As can be seen in Fig. 10, for the nanocomposites, the contrast is approximately the same, indicating that the GO particles are well dispersed throughout the polymer matrix so that an exfoliated structure is obtained. Based on the TEM micrographs along with XRD, FE-SEM and Raman results, we

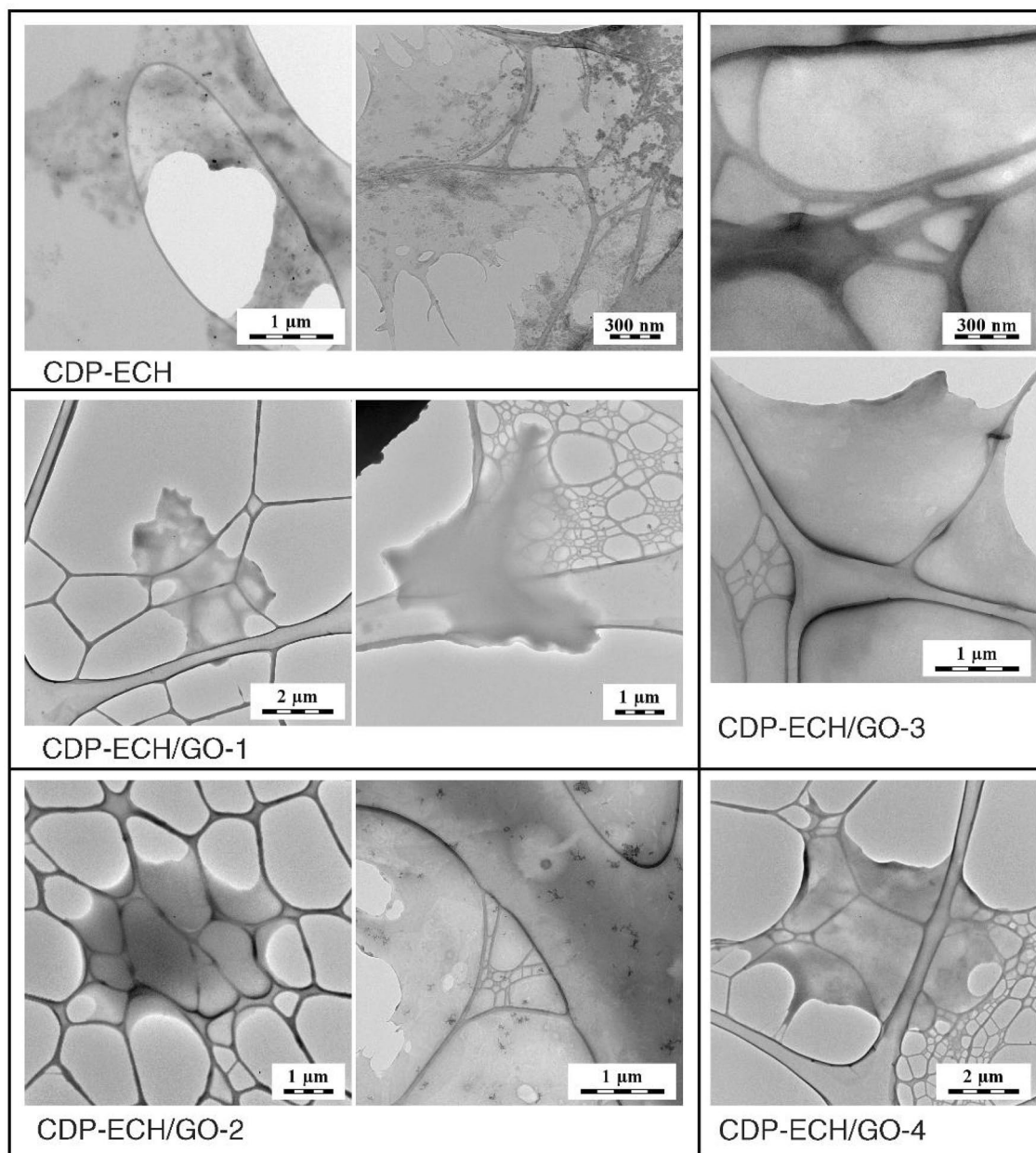


Fig. 10 TEM images of CDP-ECH, CDP-ECH/GO-1, 2, 3 and 4

can propose that a homogenised and exfoliated structure in the nanocomposites was successfully obtained.

Swelling behaviors

The swelling capacities of CDP-ECH and CDP-ECH/GOs to determine the effect of GO content on the swelling behavior of polymers were tested and the outcomes have been revealed in Fig. 11. Generally, it was shown that the swelling ratio of polymers is rising with the increase of GO content. The CDP-ECH revealed an equilibrium swelling ratio of 508%, which increased to 564% after

the incorporation 0.3% of GO. We propose that it is due to the presence of functional groups of CDP-ECH and GO for water absorption in CDP-ECH/GO-1. However, the swelling ratio decreased with the incorporation 0.6 and 1.2% of GO to 523 and 531% in the nanocomposite, respectively. This is probably due to the crosslinking action of the GO and much denser networks formed in the CDP-ECH/GO nanocomposites. In this case, the GO nanosheets act as crosslinking junctions that restrain the swelling of the CDP-ECH/GO. On the other hand, the increase in the swelling capacities of the nanocomposite containing 2.4 wt% of GO is due to growth of the density

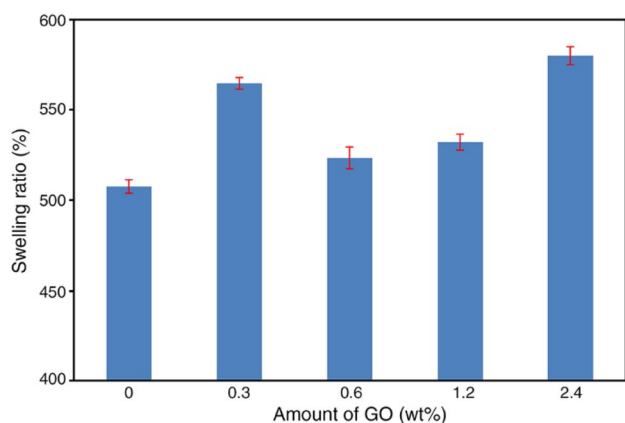


Fig. 11 Swelling capacities of CDP-ECH and its nanocomposites in water

of the hydrophilic groups in the polymer nanocomposite networks.

Adsorption test

To testify further the existence and chemical activity of GO in polymer nanocomposites, adsorption tests toward methylene blue (MB), phenol (PN, 1-naphthol (1-NPH) and 2-naphthol (2-NPH) were carried out with CDP-ECH/GO as adsorbent. For comparison, CDP-ECH was also tested under the same conditions.

The adsorption results are shown in Fig. 12, where in each case, the portion of sorbate removed from the solution (removal percentage) against the CDP-ECH and CDP-ECH/GOs is presented. As shown in Fig. 11, the CDP-ECH adsorbs MB very slightly (as a model cationic dye) due to quite hydrophilic characteristic of the adsorbate. It is well known that MB is adsorbed by this polymer in the first 30 min and then gradually went back into the solution (Zhao et al. 2009). The adsorption of MB by all of the CDP-ECH/GOs sharply increased compared to the CDP-ECH. So, the adsorption quantity of β -CD polymer nanocomposites increases along with the increase of initial GO loading. The removal percentage of MB was enhanced from 8.1 to 92.2% when β -CD polymer contained 2.4% of GO. It is inferred that for MB it is difficult to be absorbed by hydrophobic cavities of β -CD, but according to literature (Yang et al. 2011) the GO nanosheets present in nanocomposites can effectively adsorb the cationic MB through electrostatic and the π - π stacking interactions. The absorption capacity of 714 mg/g was reported for GO when the initial MB concentration was below 250 mg/L, the removal efficiency was higher than 99% (Yang et al. 2011).

The adsorption of PN, 1-NPH and 2-NPH by CDP-ECH and CDP-ECH/GO-1, 2, 3 and 4 are depicted in Fig. 12. The experimental data show that the amount of 2-NPH absorbed by CDP-ECH is higher than 1-NPH and these are higher than that of PN. Naphthalene derivatives due to molecular size are more suitable than phenol for the formation of β -CD inclusion complex, thus, the adsorption toward naphthalene

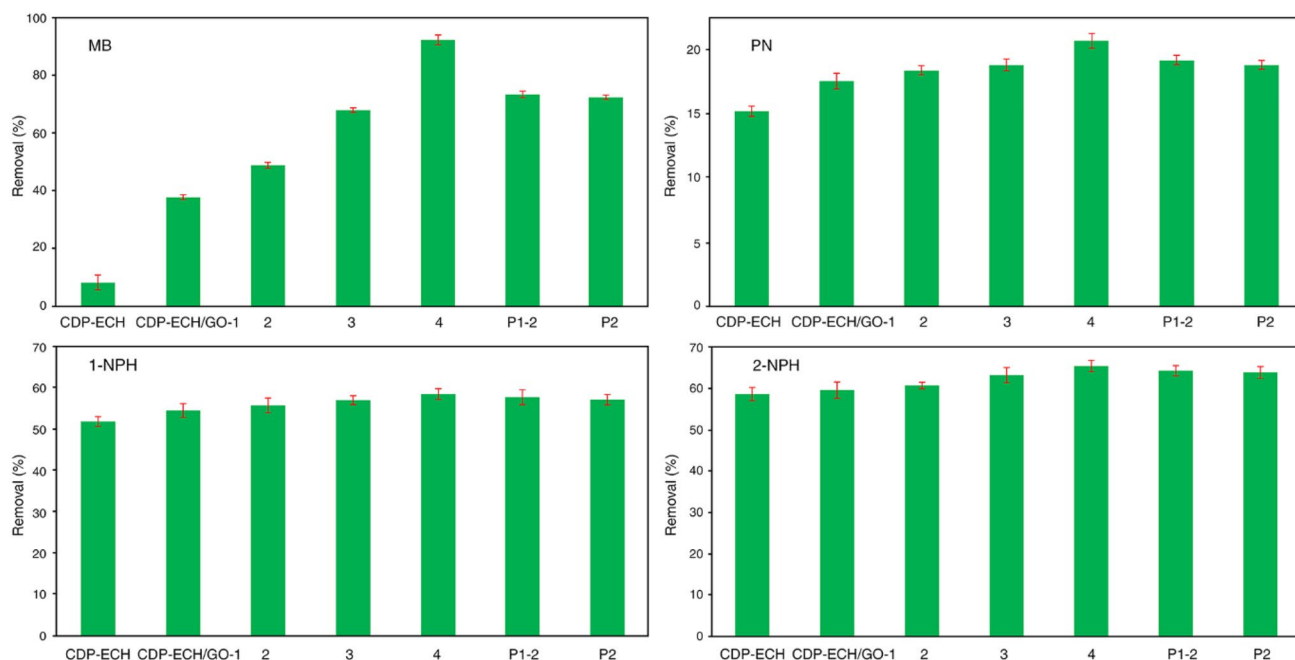


Fig. 12 Absorption of methylene blue (MB), phenol (PN), 1-naphthol (1-NPH) and 2-naphthol (2-NPH) by CDP-ECH and its nanocomposites [$C_0 = 50$ (MB), 25 (PN), 100 (1-NPH) and 100 (2-NPH) mg/L, $V = 50$ mL, $T = 25$ °C, $W = 0.1$ g]

derivatives are much higher than PN. On the other hand, the 2-NPH forms a more stable inclusion complex with β -CD in comparison with 1-NPH, due to the steric hindrance of 1-NPH. As illustrated in Fig. 12, the adsorption of these sorbates by β -CD polymer nanocomposites is higher than β -CD polymer. So, adsorption of PN in the GO sheets of nanocomposites seems to be more important than that of 1-NPH and 2-NPH. The main sorption mechanism of phenol and naphthalene derivatives in the β -CD polymer is inclusion within the β -CD cavities and the polymer networks, consequently, the existence of GO nanosheets in nanocomposites represent additional sites for absorption of aromatic organic molecules. It is well documented that the reason is due to the π - π interaction between graphene sheets and the adsorbed materials and the absorption capacity of 133.8 and 346 mg/g were reported for phenol and 1-naphthol, respectively (Li et al. 2012; Pei et al. 2013; Wang et al. 2014; Zhao et al. 2011a). The adsorption capacity of 2-naphthol estimated equal to the value of a corresponding amount of 1-naphthol (Pei et al. 2013). As a result, a synergic effect is found for CDP-ECH/GO nanocomposites: the β -CD moieties, the network structures and GO nanosheets which contribute to the higher amount of absorbed guest molecules. The results of adsorption tests confirmed the existence and chemical activity of GO nanosheets in CDP-ECH/GO. In addition, the results disclosed that the GO presence results in higher adsorption ability of β -CD polymer, especially for cationic adsorbates.

As seen in the Fig. 12, the experimental data show that the amount of absorbed materials by nanocomposite which prepared by Path 1–2 (CDP-ECH/GO-P1–2) is slightly higher than that for both nanocomposite by path 1–1 (CDP-ECH/GO-3) and also by path 2 (CDP-ECH/GO-P2). It demonstrates the presence of the more covalent bonds between β -CD, GO nanosheets and ECH and much denser networks in the CDP-ECH/GO-3 in comparison with CDP-ECH/GO-P1–2 and P2.

Conclusions

An environmentally friendly and facile method was developed to prepare macromolecule nanocomposites containing β -CD and GO. The β -CD was successfully polymerized in an aqueous solution of GO using ECH as a crosslinker. Both structural and morphological analyses showed uniform distribution of GO in the polymer matrix through covalent linkage. Due to the high surface area effect of GO and multi-site characteristic of CDP-ECH in the obtained nanocomposites, it can be concluded that CDP-ECH/GO acts as potential low-cost and efficient sorbents for removal hazardous materials from the environment. Consequently, the absorption into the nanocomposites increased in comparison with CDP-ECH.

Therefore, these reported novel materials have a potential to become biocompatible macromolecules for a variety of technological applications, such as biomedical engineering, construction engineering and hygienic products.

Acknowledgements The authors gratefully acknowledge the Faculty Research Committee of Shahid Bahonar University of Kerman for financial support of this project. One of the authors (ICH) is grateful for support from the project VEGA 2/0108/14.

Compliance with ethical standards

Conflict of interest The authors declare that they have no conflict of interest.

References

- Allen MJ, Tung VC, Kaner RB (2010) Honeycomb carbon: a review of graphene. *Chem Rev* 110:132–145. <https://doi.org/10.1021/cr900070d>
- Alsaibee A, Smith BJ, Xiao L, Ling Y, Helbling DE, Dichtel WR (2016) Rapid removal of organic micropollutants from water by a porous beta-cyclodextrin polymer. *Nature* 529:190–194. <https://doi.org/10.1038/nature16185>
- Chen D, Feng H, Li J (2012a) Graphene oxide: preparation, functionalization, and electrochemical applications. *Chem Rev* 112:6027–6053. <https://doi.org/10.1021/cr300115g>
- Chen L, Hu P, Zhang L, Huang S, Luo L, Huang C (2012b) Toxicity of graphene oxide and multi-walled carbon nanotubes against human cells and zebrafish. *Sci China Chem* 55:2209–2216. <https://doi.org/10.1007/s11426-012-4620-z>
- Chen JT et al (2013) Tuning nanostructure of graphene oxide/polyelectrolyte LbL assemblies by controlling pH of GO suspension to fabricate transparent and super gas barrier films. *Nanoscale* 5:9081–9088. <https://doi.org/10.1039/c3nr02845c>
- Chen X, Zhou S, Zhang L, You T, Xu F (2016) Adsorption of heavy metals by graphene oxide/cellulose hydrogel prepared from NaOH/urea aqueous solution materials (Basel) 9:582. <https://doi.org/10.3390/ma9070582>
- Crini G et al (1998) Solid state NMR spectroscopy study of molecular motion in cyclomaltoheptaose (beta-cyclodextrin) crosslinked with epichlorohydrin. *Carbohydr Res* 308:37–45. [https://doi.org/10.1016/s0008-6215\(98\)00077-9](https://doi.org/10.1016/s0008-6215(98)00077-9)
- Deng X, Lu L, Li H, Luo F (2010) The adsorption properties of Pb(II) and Cd(II) on functionalized graphene prepared by electrolysis method. *J Hazard Mater* 183:923–930. <https://doi.org/10.1016/j.jhazmat.2010.07.117>
- Eom D et al (2009) Structure and electronic properties of graphene nanoislands on Co(0001). *Nano Lett* 9:2844–2848. <https://doi.org/10.1021/nl900927f>
- Fenyvesi E, Gruiz K, Verstichel S, De Wilde B, Leitgeb L, Csabai K, Szaniszló N (2005) Biodegradation of cyclodextrins in soil. *Chemosphere* 60:1001–1008. <https://doi.org/10.1016/j.chemosphere.2005.01.026>
- Gaffar MA, El-Rafie SM, El-Tahawy KF (2004) Preparation and utilization of ionic exchange resin via graft copolymerization of β -CD itaconate with chitosan. *Carbohydr Polym* 56:387–396. <https://doi.org/10.1016/j.carbpol.2004.01.007>
- Garcia-Zubiri IX, Gonzalez-Gaitano G, Isasi JR (2006) Thermal stability of solid dispersions of naphthalene derivatives with β -cyclodextrin and β -cyclodextrin polymers. *Thermochim Acta* 444:57–64. <https://doi.org/10.1016/j.tca.2006.02.024>

- Guo Y, Guo S, Ren J, Zhai Y, Dong S, Wang E (2010) Cyclodextrin functionalized graphene nanosheets with high supramolecular recognition capability: synthesis and host-guest inclusion for enhanced electrochemical performance. *ACS Nano* 4:4001–4010. <https://doi.org/10.1021/nn100939n>
- Guo Y, Chen Y, Zhao Q, Shuang S, Dong C (2011a) Electrochemical sensor for ultrasensitive determination of doxorubicin and methotrexate based on cyclodextrin-graphene hybrid nanosheets. *Electroanalysis* 23:2400–2407. <https://doi.org/10.1002/elan.201100259>
- Guo Y, Guo S, Li J, Wang E, Dong S (2011b) Cyclodextrin-graphene hybrid nanosheets as enhanced sensing platform for ultrasensitive determination of carbendazim. *Talanta* 84:60–64. <https://doi.org/10.1016/j.talanta.2010.12.007>
- Guo H, Jiao T, Zhang Q, Guo W, Peng Q, Yan X (2015a) Preparation of graphene oxide-based hydrogels as efficient dye adsorbents for wastewater treatment. *Nanoscale Res Lett* 10:931. <https://doi.org/10.1186/s11671-015-0931-2>
- Guo Y, Duan B, Cui L, Zhu P (2015b) Construction of chitin/graphene oxide hybrid hydrogels. *Cellulose* 22:2035–2043. <https://doi.org/10.1007/s10570-015-0630-2>
- He H, Klinowski J, Forster M, Lerf A (1998) A new structural model for graphite oxide. *Chem Phys Lett* 287:53–56. [https://doi.org/10.1016/S0009-2614\(98\)00144-4](https://doi.org/10.1016/S0009-2614(98)00144-4)
- Heydari A, Sheibani H (2015) Fabrication of poly(β -cyclodextrin-co-citric acid)/bentonite clay nanocomposite hydrogel: thermal and absorption properties. *RSC Adv* 5:82438–82449. <https://doi.org/10.1039/c5ra12423a>
- Heydari A, Sheibani H (2016) Facile polymerization of β -cyclodextrin functionalized graphene or graphene oxide nanosheets using citric acid crosslinker by in situ melt polycondensation for enhanced electrochemical performance. *RSC Adv* 6:9760–9771. <https://doi.org/10.1039/c5ra24685g>
- Heydari A, Iranmanesh M, Doostan F, Sheibani H (2015) Preparation of inclusion complex between nifedipine and ethylenediamine- β -cyclodextrin as nanocarrier agent. *Pharm Chem J* 49:605–612. <https://doi.org/10.1007/s11094-015-1338-1>
- Heydari A, Doostan F, Khoshnood H, Sheibani H (2016) Water-soluble cationic poly(β -cyclodextrin-co-guanidine) as a controlled vitamin B2 delivery carrier. *RSC Adv* 6:33267–33278. <https://doi.org/10.1039/c6ra01011c>
- Heydari A, Hassani Y, Sheibani H, Pardakhti A (2017a) Water-soluble β -cyclodextrin polymers as drug carriers to improve solubility, thermal stability and controlled release of nifedipine. *Pharm Chem J* 51:375–383. <https://doi.org/10.1007/s11094-017-1617-0>
- Heydari A, Khoshnood H, Sheibani H, Doostan F (2017b) Polymerization of β -cyclodextrin in the presence of bentonite clay to produce polymer nanocomposites for removal of heavy metals from drinking water. *Polym Adv Technol* 28:524–532. <https://doi.org/10.1002/pat.3951>
- Heydari A, Pardakhti A, Sheibani H (2017c) Preparation and characterization of zwitterionic poly(β -cyclodextrin-co-guanidinocitrate) hydrogels for ciprofloxacin controlled release. *Macromol Mater Eng* 302:1600501. <https://doi.org/10.1002/mame.201600501>
- Hong BJ, Compton OC, An Z, Eryazici I, Nguyen ST (2012) Successful stabilization of graphene oxide in electrolyte solutions: enhancement of biofunctionalization and cellular uptake. *ACS Nano* 6:63–73. <https://doi.org/10.1021/nn202355p>
- Hummers WS, Offeman RE (1958) Preparation of graphitic oxide. *J Am Chem Soc* 80:1339. <https://doi.org/10.1021/ja01539a017>
- Lee PS, Han JY, Song TW, Sung JH, Kwon OS, Song S, Chung YB (2006) Physicochemical characteristics and bioavailability of a novel intestinal metabolite of ginseng saponin (IH901) complexed with β -cyclodextrin. *Int J Pharm* 316:29–36. <https://doi.org/10.1016/j.ijpharm.2006.02.035>
- Lee C, Wei X, Kysar JW, Hone J (2008) Measurement of the elastic properties and intrinsic strength of monolayer graphene. *Science* 321:385–388. <https://doi.org/10.1126/science.1157996>
- Lerf A, He H, Forster M, Klinowski J (1998) Structure of graphite oxide revisited. *J Phys Chem B* 102:4477–4482. <https://doi.org/10.1021/jp9731821>
- Li Y et al (2011) Adsorption of fluoride from aqueous solution by graphene. *J Colloid Interface Sci* 363:348–354. <https://doi.org/10.1016/j.jcis.2011.07.032>
- Li Y et al (2012) Equilibrium, kinetic and thermodynamic studies on the adsorption of phenol onto graphene. *Mater Res Bull* 47:1898–1904. <https://doi.org/10.1016/j.materresbull.2012.04.021>
- Liu K, Wei J, Wang C (2011) Sensitive detection of rutin based on β -cyclodextrin@chemically reduced graphene/Nafion composite film. *Electrochim Acta* 56:5189–5194. <https://doi.org/10.1016/j.electacta.2011.03.042>
- Liu Z, Ma X, Zhang H, Lu W, Ma H, Hou S (2012) Simultaneous determination of nitrophenol isomers based on β -cyclodextrin functionalized reduced graphene oxide. *Electroanalysis* 24:1178–1185. <https://doi.org/10.1002/elan.201100735>
- Liu J-W, Yang T, Chen S, Chen X-W, Wang J-H (2013) Nickel chelating functionalization of graphene composite for metal affinity membrane isolation of lysozyme. *J Mater Chem B* 1:810–818. <https://doi.org/10.1039/C2TB00334A>
- Liu J, Liu G, Liu W (2014) Preparation of water-soluble β -cyclodextrin/poly(acrylic acid)/graphene oxide nanocomposites as new adsorbents to remove cationic dyes from aqueous solutions. *Chem Eng J* 257:299–308. <https://doi.org/10.1016/j.cej.2014.07.021>
- Liu J, Liu G, Liu W, Wang Y, Xu M, Wang B (2016) Turn-on fluorometric β -carotene assay based on competitive host-guest interaction between rhodamine 6G and β -carotene with a graphene oxide functionalized with a β -cyclodextrin-modified polyethyleneimine. *Microchim Acta* 183:1161–1168. <https://doi.org/10.1007/s00604-016-1747-1>
- Loftsson T, Brewster ME (1996) Pharmaceutical applications of cyclodextrins. 1. Drug solubilization and stabilization. *J Pharm Sci* 85:1017–1025. <https://doi.org/10.1021/js950534b>
- Mishra AK, Ramaprabhu S (2011) Functionalized graphene sheets for arsenic removal and desalination of sea water. *Desalination* 282:39–45. <https://doi.org/10.1016/j.desal.2011.01.038>
- Mocanu G, Vizitiu D, Carпов A (2001) Cyclodextrin polymers. *J Bioact Compat Polym* 16:315–342. <https://doi.org/10.1106/JJUV-8F2K-JGYF-HNGF>
- Morin-Crini N, Crini G (2013) Environmental applications of water-insoluble β -cyclodextrin-epichlorohydrin polymers. *Prog Polym Sci* 38:344–368. <https://doi.org/10.1016/j.progpolymsci.2012.06.005>
- Namazi H, Heydari A (2014) Synthesis of β -cyclodextrin-based dendrimer as a novel encapsulation agent. *Polym Int* 63:1447–1455. <https://doi.org/10.1002/pi.4637>
- Namazi H, Fathi F, Heydari A (2012) Nanoparticles based on modified polysaccharides. In: Hashim A (ed) *The delivery of nanoparticles*. InTech, Rijeka, pp 149–184. <https://doi.org/10.5772/34795>
- Namazi H, Heydari A, Pourfarzolla A (2014) Synthesis of glycoconjugated polymer based on polystyrene and nanoporous β -cyclodextrin to remove copper (II) from water pollution. *Int J Polym Mater Polym Biomater* 63:1–6. <https://doi.org/10.1080/00914037.2013.769240>
- Pei Z, Li L, Sun L, Zhang S, Shan X-Q, Yang S, Wen B (2013) Adsorption characteristics of 1,2,4-trichlorobenzene, 2,4,6-trichlorophenol, 2-naphthol and naphthalene on graphene and graphene oxide. *Carbon* 51:156–163. <https://doi.org/10.1016/j.carbon.2012.08.024>
- Pitha J, Rao CT, Lindberg B, Seffers P (1990) Distribution of substituents in 2-hydroxypropyl ethers of cyclomaltoheptaose. *Carbohydr Res* 200:429–435. [https://doi.org/10.1016/0008-6215\(90\)84208-c](https://doi.org/10.1016/0008-6215(90)84208-c)

- Prabaharan M, Mano JF (2006) Chitosan derivatives bearing cyclodextrin cavities as novel adsorbent matrices. *Carbohydr Polym* 63:153–166. <https://doi.org/10.1016/j.carbpol.2005.08.051>
- Pratt DY, Wilson LD, Kozinski JA, Mohart AM (2010) Preparation and sorption studies of β -cyclodextrin/epichlorohydrin copolymers. *J Appl Polym Sci* 116:2982–2989. <https://doi.org/10.1002/app.31824>
- Qi Y, Yang M, Xu W, He S, Men Y (2017) Natural polysaccharides-modified graphene oxide for adsorption of organic dyes from aqueous solutions. *J Colloid Interface Sci* 486:84–96. <https://doi.org/10.1016/j.jcis.2016.09.058>
- Ramesha GK, Kumara AV, Muralidhara HB, Sampath S (2011) Graphene and graphene oxide as effective adsorbents toward anionic and cationic dyes. *J Colloid Interface Sci* 361:270–277. <https://doi.org/10.1016/j.jcis.2011.05.050>
- Renard E, Deratani A, Volet G, Sebille B (1997) Preparation and characterization of water soluble high molecular weight β -cyclodextrin-epichlorohydrin polymers. *Eur Polym J* 33:49–57. [https://doi.org/10.1016/S0014-3057\(96\)00123-1](https://doi.org/10.1016/S0014-3057(96)00123-1)
- Singh M, Sharma R, Banerjee UC (2002) Biotechnological applications of cyclodextrins. *Biotechnology advances* 20:341–359. [https://doi.org/10.1016/S0734-9750\(02\)00020-4](https://doi.org/10.1016/S0734-9750(02)00020-4)
- Stankovich S et al (2007) Synthesis of graphene-based nanosheets via chemical reduction of exfoliated graphite oxide. *Carbon* 45:1558–1565. <https://doi.org/10.1016/j.carbon.2007.02.034>
- Tan L, Zhou K-G, Zhang Y-H, Wang H-X, Wang X-D, Guo Y-F, Zhang H-L (2010) Nanomolar detection of dopamine in the presence of ascorbic acid at β -cyclodextrin/graphene nanocomposite platform. *Electrochem Commun* 12:557–560. <https://doi.org/10.1016/j.elec.2010.01.042>
- Wang X, Huang S, Zhu L, Tian X, Li S, Tang H (2014) Correlation between the adsorption ability and reduction degree of graphene oxide and tuning of adsorption of phenolic compounds. *Carbon* 69:101–112. <https://doi.org/10.1016/j.carbon.2013.11.070>
- Wang S, Li Y, Fan X, Zhang F, Zhang G (2016) β -Cyclodextrin functionalized graphene oxide: an efficient and recyclable adsorbent for the removal of dye pollutants. *Front Chem Sci Eng* 9:77–83. <https://doi.org/10.1007/s11705-014-1450-x>
- Xu C, Wang J, Wan L, Lin J, Wang X (2011) Microwave-assisted covalent modification of graphene nanosheets with hydroxypropyl- β -cyclodextrin and its electrochemical detection of phenolic organic pollutants. *J Mater Chem* 21:10463. <https://doi.org/10.1039/c1jm10478k>
- Yan T, Zhang H, Huang D, Feng S, Fujita M, Gao XD (2017) Chitosan-Functionalized Graphene Oxide as a Potential Immunoadjuvant. *Nanomaterials (Basel)* 7:59. <https://doi.org/10.3390/nano7030059>
- Yang ST et al (2010a) Folding/aggregation of graphene oxide and its application in Cu^{2+} removal. *J Colloid Interface Sci* 351:122–127. <https://doi.org/10.1016/j.jcis.2010.07.042>
- Yang X, Li L, Shang S, Tao X (2010b) Synthesis and characterization of layer-aligned poly(vinyl alcohol)/graphene nanocomposites. *Polymer* 51:3431–3435. <https://doi.org/10.1016/j.polymer.2010.05.034>
- Yang ST, Chen S, Chang Y, Cao A, Liu Y, Wang H (2011) Removal of methylene blue from aqueous solution by graphene oxide. *J Colloid Interface Sci* 359:24–29. <https://doi.org/10.1016/j.jcis.2011.02.064>
- Zhao D, Zhao L, Zhu CS, Shen X, Zhang X, Sha B (2009) Comparative study of polymer containing β -cyclodextrin and -COOH for adsorption toward aniline, 1-naphthylamine and methylene blue. *J Hazard Mater* 171:241–246. <https://doi.org/10.1016/j.jhazmat.2009.05.134>
- Zhao X, Zhang Q, Chen D (2010) Enhanced mechanical properties of graphene-based poly(vinyl alcohol) composites. *Macromolecules* 43:2357–2363. <https://doi.org/10.1021/ma902862u>
- Zhao G, Jiang L, He Y, Li J, Dong H, Wang X, Hu W (2011a) Sulfonated graphene for persistent aromatic pollutant management. *Adv Mater* 23:3959–3963. <https://doi.org/10.1002/adma.201101007>
- Zhao G, Li J, Wang X (2011b) Kinetic and thermodynamic study of 1-naphthol adsorption from aqueous solution to sulfonated graphene nanosheets. *Chem Eng J* 173:185–190. <https://doi.org/10.1016/j.cej.2011.07.072>